Two-component parton fractional quantum Hall state in graphene

Ying-Hai Wu *

School of Physics and Wuhan National High Magnetic Field Center, Huazhong University of Science and Technology, Wuhan 430074, China

(Received 12 July 2022; revised 21 September 2022; accepted 7 October 2022; published 18 October 2022)

We study the $\nu = \pm 1/2$ fractional quantum Hall states in graphene observed by Zibrov *et al.* [A. A. Zibrov, E. M. Spanton, H. Zhou, C. Kometter, T. Taniguchi, K. Watanabe, and A. F. Young, Nat. Phys. **14**, 930 (2018)]. The parton construction is employed to provide a valley unpolarized trial wave function for these states. The lattice scale valley anisotropic terms in the Hamiltonian soften the repulsion between electrons in different valleys to favor the valley unpolarized state. The validity of our proposal is corroborated by numerical calculations.

DOI: 10.1103/PhysRevB.106.155132

I. INTRODUCTION

The extraordinary properties of graphene and other two-dimensional materials have sparked intensive research activities on these systems. One fruitful line of investigation is about strongly correlated many-body states in high magnetic field [1,2], for which the fractional quantum Hall (FQH) effect is a prominent example [3]. The experimental signature of FQH effect in electric transport is quantized Hall resistance accompanied by exponentially suppressed longitudinal resistance. The application of an external magnetic field generates discrete Landau levels (LLs) for the electrons, where all single-particle orbitals in the same level have the same kinetic energy. If one Landau level is partially populated and electron-electron interactions are absent, there is an exponential degeneracy in the many-body spectrum. It is a great surprise that interactions would lead to energy gaps at certain filling factors ν (i.e., the number of electrons divided by the number of orbitals in each LL) [4–8].

The most extensively used platform for studying FQH states has been two-dimensional electron gases (2DEGs) in GaAs based structures. A variety of FQH states have also been revealed in graphene and its multilayers thanks to substantial progress in sample fabrication [9–24]. The characteristics of graphene that distinguish it from conventional 2DEG include its Dirac dispersion, the fourfold spin and valley degeneracy, and direct access to the two-dimensional plane by experimental probes. The Dirac dispersion and valley degree of freedom endow the single-particle wave functions in the LLs with a spinor structure, which leads to effective interaction that could favor exotic FQH states with non-Abelian anyons [21]. The long-range Coulomb interaction is SU(4) symmetric in the spin-valley space, but one generally expects spontaneous symmetry breaking such that the many-body states are spin and/or valley polarized. In addition, there are are lattice scale interactions that break the SU(4) spin-valley symmetry. The interplay of these effects has been analyzed to explain why some FQH states are missing or very weak in certain experiments [12,25,26].

This paper focuses on the $\nu = \pm 1/2$ FQH states in the zeroth LL of graphene [20]. To elucidate its nature, the first question is whether it is one-component or multicomponent. In the former case, an odd denominator rule has been firmly established, which can be explained very well using the composite fermion theory [7]. An exception to this rule is the 5/2 state in the second LL of GaAs [27], which could harbor non-Abelian Ising anyons described by the Moore-Read state or its variants [8,28–46], but it is not likely to be relevant in the zeroth LL of graphene because the projected interaction here is quite different from that in the second LL of GaAs. For bilayer systems made of GaAs or graphene, even-denominator FQH states have been observed in many experiments [22,23,47,48], which can be understood using two-component Halperin and Jain wave functions [6,49–52]. As we shall argue below, the Halperin state is not really a plausible candidate for the states observed in monolayer graphene.

Instead, we propose that the experimental observation can be understood using the parton theory. The basic idea is to break one electron into multiple fermionic partons and each of them form an integer quantum Hall (IQH) state (or some other mean-field states in general) [53]. The partons are not completely free and should be glued together by emergent gauge fields [54]. In spite of the elegance and generality of this approach, it does not seem to be relevant to actual quantum Hall physics for a long time. The composite fermion theory can be viewed as a special case of the parton construction, but this reinterpretation does not bring out particularly useful insights. In recent years, several works have found that some one-component parton FQH states might be realized in bilayer graphene [55], graphene [21], and second LL or wide quantum wells of GaAs [56–60]. In contrast, this paper aims to show that a two-component parton FQH state was realized in Ref. [20]. This state was originally constructed in Ref. [53] and tested as a candidate for the 5/2 state in GaAs [61,62]. At present, most experimental and numerical results on the 5/2 state suggest that it is actually spin polarized [28,34,63–66], so the two-component state is not likely relevant. It was proposed that

*yinghaiwu88@hust.edu.cn

this state features d-wave pairing [67]. We also note that an explanation completely different from ours has been proposed in Ref. [68].

The rest of this paper is organized as follows. In Sec. II, we introduce the model for graphene with valley anisotropic terms in the Hamiltonian. In Sec. III, we describe the parton FQH state and demonstrate that it could be realized in certain parameter regimes. The paper is concluded in Sec. IV.

II. MODELS

We consider a graphene sheet in the x-y plane with the two Dirac cones denoted as K^+ and K^-. An external magnetic field is applied along the z direction so the single-particle Hamiltonians in the two valleys are

$$H_0^{\pm} = v_{\mathrm{F}} \begin{bmatrix} 0 & \pi_x \pm i\pi_y \\ \pi_x \mp i\pi_y & 0 \end{bmatrix}, \tag{1}$$

where v_{F} is the Fermi velocity and $\pi_{x,y}$ are the canonical momentum operators. The zeroth LL of graphene includes the zero-energy single-particle eigenstates

$$\begin{bmatrix} \phi_m \\ 0 \end{bmatrix} \tag{2}$$

in the K^+ valley and

$$\begin{bmatrix} 0 \\ \phi_m \end{bmatrix} \tag{3}$$

in the K^- valley, where ϕ_m represent the wave functions in the lowest LL of nonrelativistic particles. It is customary to consider an infinite plane with electromagnetic vector potential $A = (-By/2, Bx/2, 0)$. In this case, the argument of ϕ_m is the complex coordinate $z = x + iy$ and m labels its angular momentum. Numerical calculations are commonly performed on the sphere rather than the disk because there is no complication due to open boundary [5]. A radial magnetic field through the surface of the sphere is generated by a magnetic monopole at the center. The single-particle wave functions are labeled by the total angular momentum and its z component [69,70].

The zeroth LL is of our interest and all operators in the subsequent discussions are projected to it. The kinetic energy is a constant that may be neglected. The interaction Hamiltonian can be separated to the long-range Coulomb potential

$$V(\mathbf{r} - \mathbf{r}') = \frac{1}{|\mathbf{r} - \mathbf{r}'|} \tag{4}$$

that respects the SU(4) spin-valley symmetry and some other terms that break this symmetry [25]. The spin rotation symmetry is broken by the Zeeman coupling and the valley symmetry is broken by the following two terms:

$$\begin{aligned} H_{\mathrm{VA}}^{z} &= \frac{g_z}{2} \int d\mathbf{r} : [\widehat{\Psi}^{\dagger}(\mathbf{r}) \tau^z \widehat{\Psi}(\mathbf{r})]^2 :, \\ H_{\mathrm{VA}}^{\perp} &= \frac{g_{\perp}}{2} \int d\mathbf{r} \sum_{\alpha=x,y} : [\widehat{\Psi}^{\dagger}(\mathbf{r}) \tau^{\alpha} \widehat{\Psi}(\mathbf{r})]^2 :, \end{aligned} \tag{5}$$

where the electron creation operator $\widehat{\Psi}^{\dagger}(\mathbf{r})$ is a four-component spinor:

$$[\widehat{\psi}^{\dagger}_{K^+\uparrow}(\mathbf{r}), \widehat{\psi}^{\dagger}_{K^+\downarrow}(\mathbf{r}), \widehat{\psi}^{\dagger}_{K^-\uparrow}(\mathbf{r}), \widehat{\psi}^{\dagger}_{K^-\downarrow}(\mathbf{r})]. \tag{6}$$

H_{VA}^{z} arises from electron-electron interactions and $H_{\mathrm{VA}}^{\perp}$ arises from both electron-electron and electron-phonon interactions [71–73]. We note that there are fewer terms here compared to the general results because the single-particle eigenstates have only one nonzero component. The valley anisotropic terms only penalize two electrons that coincide in space. In other words, their valley indices make a difference if the distance between them is comparable to the lattice constant. It is helpful to express the Hamiltonian using the Haldane pseudopotentials $\mathcal{P}_{ij}(\mathrm{RAM})$ [5], which characterize the energy cost associated with putting two electrons in definite relative angular momentum (RAM) states. The Coulomb potential is decomposed to a summation of pseudopotentials in all possible RAM channels, but the valley anisotropic terms only generate the pseudopotential with zero RAM [26]. The Pauli principle forbids two electrons with the same spin and valley indices to have zero RAM, so the valley anisotropic terms only penalize two electrons with different spin and/or valley indices.

A full description of the zeroth LL physics is quite involved, and the model should be simplified based on experimental evidence to make it numerically tractable [20]. To begin with, the $\nu = \pm 1/2$ states are related to each other by particle-hole symmetry within the zeroth LL, so we shall only consider the $\nu = -1/2$ state. It is beneficial to inspect the $\nu = -1$ and 0 states. The $\nu = -1/2$ state can be obtained by adding electrons to the $\nu = -1$ state toward the $\nu = 0$ state. The spin and valley indices of these electrons should be chosen in such a way that the $\nu = -1$ and 0 states are connected. The $\nu = -1$ state is relatively straightforward as the Hamiltonian almost certainly favors a state with complete spin and valley polarizations. In other words, the electrons occupy the same sublevel of the zeroth LL to produce a ferromagnetic state that is expected to have the lowest energy. The nature of the $\nu = 0$ state is much more complicated. The proposed candidates include a spin polarized ferromagnetic state, a valley polarized charge density wave state, a canted antiferromagnetic state with broken spin symmetry, and a density wave with partial valley polarization [74–77]. It is quite difficult to distinguish between them in experiments. One piece of useful information is that the $\nu = -1/2$ state should be spin polarized since applying an in-plane magnetic field does not change it [20]. In contrast, there is no simple way to directly probe the valley index. The physical picture is transparent if spin or valley canting is absent [20]. When electrons are added on top of the $\nu = -1$ state, they need to populate the same valley to generate a charge density wave but the opposite valley to generate an antiferromagnet. In the transition regime between the charge density wave and the antiferromagnet, the electrons may have equal probability of occupying both valleys. This suggests that we can try to search for the $\nu = -1/2$ FQH state in a two-component system with Coulomb potential modified by the lattice scale valley anisotropic terms. In second

quantized notation, the Hamiltonian is

$$H = \frac{1}{2}\sum_{\alpha,\beta=\pm}\sum_{\{m_i\}} V_{m_1m_2m_3m_4} C^\dagger_{\alpha,m_1} C^\dagger_{\beta,m_2} C_{\beta,m_4} C_{\alpha,m_3} + \frac{F_0}{2}\sum_{\{m_i\}} W_{m_1m_2m_3m_4} C^\dagger_{+,m_1} C^\dagger_{-,m_2} C_{-,m_4} C_{+,m_3}, \quad (7)$$

where $C^\dagger_{\pm,m}$ creates an electron in the $K^\pm$ valley with index m, the coefficients $V_{m_1m_2m_3m_4}$ are derived from the Coulomb potential, and $W_{m_1m_2m_3m_4}$ are derived from the zeroth Haldane pseudopotential [5]. The energy is measured in units of $e^2/(\varepsilon\ell_B)$ with dielectric constant ε and magnetic length $\ell_B = \sqrt{\hbar c/(eB)}$. The factor F_0 is determined by microscopic physics in a complicated manner, but it will be treated as a phenomenological tunable parameter in our discussion. The eigenstates of this Hamiltonian can be computed using exact diagonalization (ED) and density matrix renormalization group (DMRG). ED is quite straightforward as it employs sparse matrix diagonalization methods to find a few low-lying eigenvalues and the associated eigenstates. DMRG is a variational method that searches for the optimal matrix product representation of the ground state [78–84]. The exponential growth of the Hilbert-space dimension limits the usage of ED, but DMRG can partially mitigate this problem. The total angular momentum L^2 and its z component L_z are conserved quantities on the sphere. It is obvious that the eigenstates of the two-component system with only Coulomb potential are SU(2) symmetric. One may worry that the valley anisotropic terms break the SU(2) symmetry, but this is not the case because electrons with the same valley index are not affected by the zeroth Haldane pseudopotential.

III. RESULTS

The total number of electrons is denoted as N_e and electrons are distributed equally in the two valleys. To distinguish them, the coordinates of electrons in the K^+ valley are denoted as $v_1, v_2, \ldots, v_{N_e/2}$ and those in the K^- valley are denoted as $w_1, w_2, \ldots, w_{N_e/2}$. It is also useful to combine and relabel them as $z_1 \equiv v_1, z_2 \equiv v_2, \ldots, z_{N_e/2} \equiv v_{N_e/2}, z_{N_e/2+1} \equiv w_1, z_{N_e/2+2} \equiv w_2, \ldots, z_{N_e} \equiv w_{N_e/2}$. The FQH state to be investigated is

$$\Phi \sim [\chi_1(\{v\})\chi_1(\{w\})]\chi_2(\{z\})\chi_1(\{z\}), \quad (8)$$

which occurs on the sphere at the monopole flux $N_\phi = 2N_e - 4$ [53]. The number 4 is called the shift and the ratio N_e/N_ϕ is not exactly $1/2$ in finite size systems. This wave function can be interpreted using the parton theory as illustrated in Fig. 1. One electron is decomposed to three types of partons $A, B,$ and C that carry charges $e/4$, $e/4$, and $e/2$, respectively. The A type partons inherit the valley index of the electrons while the B and C type partons do not carry such an index. In other words, the electron creation operator is rewritten as

$$\begin{bmatrix}\hat\psi^\dagger_{K^+}(\mathbf{r})\\ \hat\psi^\dagger_{K^-}(\mathbf{r})\end{bmatrix} = \begin{bmatrix}\hat\psi^\dagger_{A,K^+}(\mathbf{r})\\ \hat\psi^\dagger_{A,K^-}(\mathbf{r})\end{bmatrix} \hat\psi^\dagger_B(\mathbf{r})\, \hat\psi^\dagger_C(\mathbf{r}). \quad (9)$$

The two components of the A type partons form the $\nu = 1$ IQH states $\chi_1(\{v\})$ and $\chi_1(\{w\})$, the B type partons form the $\nu = 2$ IQH state $\chi_2(\{z\})$, and the C type partons form

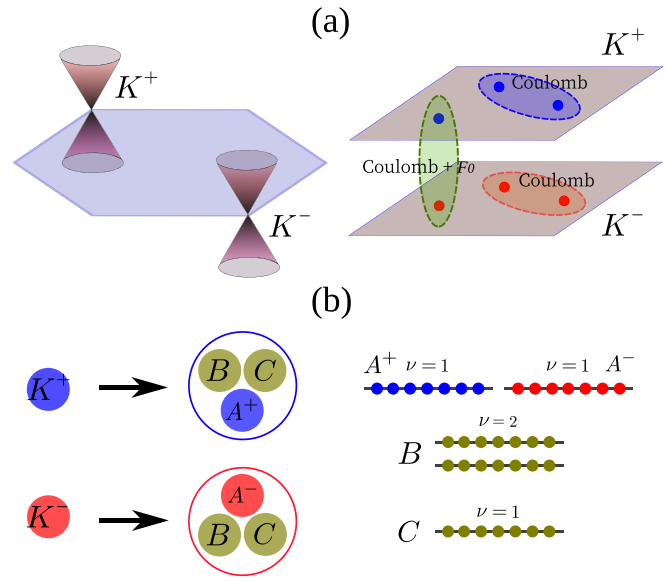

FIG. 1. Schematics of the valley unpolarized parton state in graphene. (a) In addition to the long-range Coulomb interaction, there is a short-range valley anisotropic interaction between electrons in different valleys. (b) The electrons are decomposed to partons that form their respective IQH states.

the $\nu = 1$ IQH state $\chi_1(\{z\})$. The elementary quasihole and quasiparticle of the state should carry charge $e/4$. To see this, one may increase the magnetic flux by one unit on top of the ground state. Because the state has filling factor $1/2$ and is incompressible, this operation creates a localized object with charge $e/2$. In the parton framework, one quasihole was created in both the $\chi_1(\{v\})$ and $\chi_1(\{w\})$ factors or two quasiholes were created in the $\chi_2(\{z\})$ factor. The total charge of two quasiholes is $e/2$ so each one has $e/4$.

The many-body state Eq. (8) is not completely in the lowest LL, to which it should be projected in numerical calculations. This is why we have used a $\sim$ sign instead of an equal sign because there are different approaches to the projection [85–87]. We have considered two different projection methods given by

$$\Phi_1 = \mathcal{P}_{\rm LLL}\{[\chi_1(\{v\})\chi_1(\{w\})]\chi_2(\{z\})\chi_1(\{z\})\} \quad (10)$$

and

$$\Phi_2 = [\chi_1(\{v\})\chi_1(\{w\})]\mathcal{P}_{\rm LLL}[\chi_2(\{z\})\chi_1(\{z\})]. \quad (11)$$

The first one means that we multiply the three IQH states of partons, expand it in the Fock space basis, and drop the terms that are not completely inside the lowest LL. The second one means that we multiply the two IQH states of B and C partons, expand it in the Fock space basis, drop the terms that are not completely inside the lowest LL, and then multiply it with the IQH state of A partons. These calculations are very time consuming so we have only reached $N_e = 10$ for Φ_1 and $N_e = 12$ for Φ_2. One can claim with certain confidence that both wave functions capture identical topological properties, but it is not *a priori* clear which one has better overlap with exact eigenstates of a specific Hamiltonian. In fact, it is possible that two wave functions in the same universality class have negligible overlap. The overlaps between Φ_1 (Φ_2) and

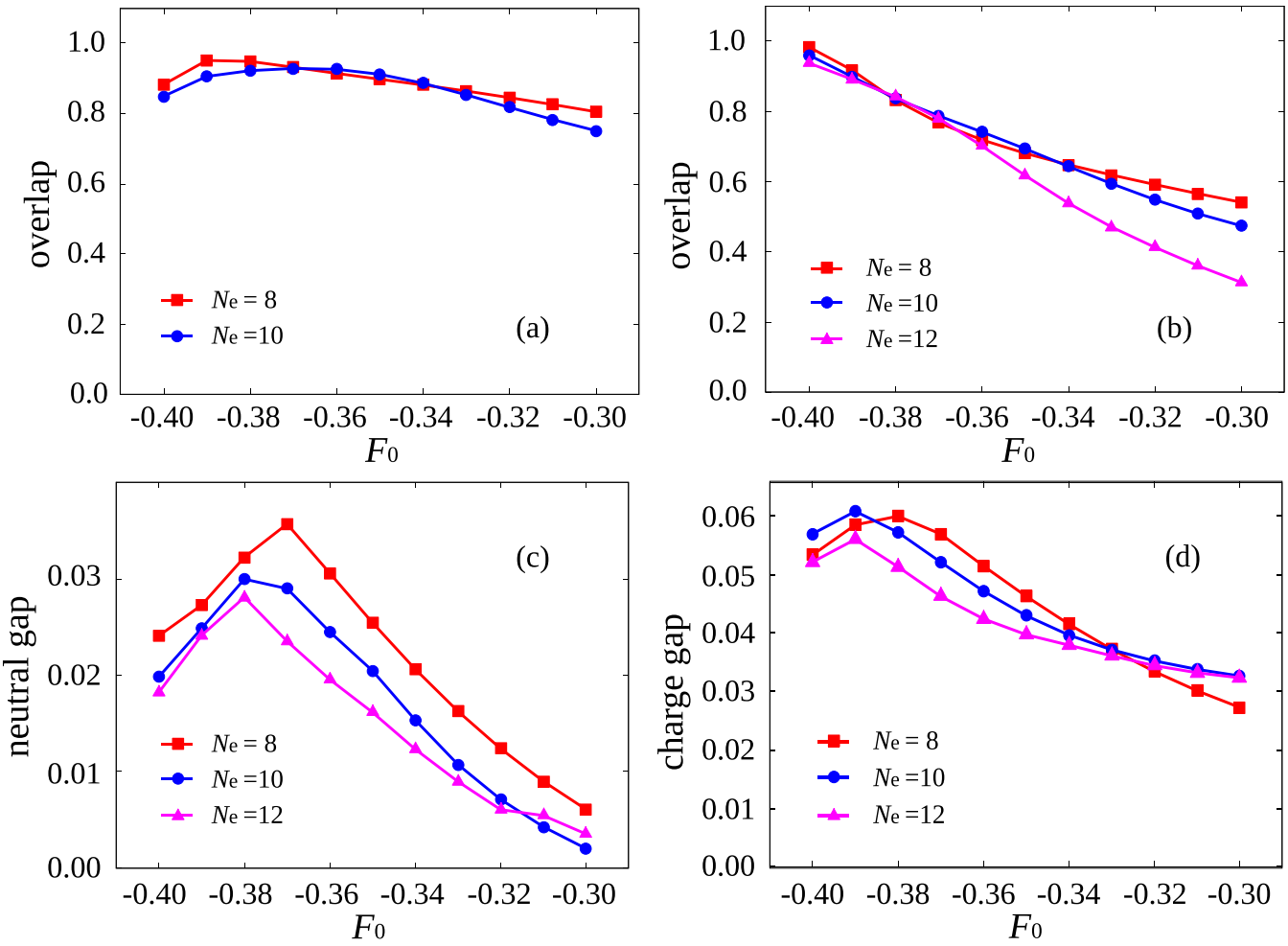

FIG. 2. Exact diagonalization results for the cases with $N_e = 8, 10, 12$ and $F_0 \in [-0.40, -0.30]$. (a) The overlap between Φ_1 in Eq. (10) and the exact ground state. (b) The overlap between Φ_2 in Eq. (11) and the exact ground state. (c) The neutral gap Δ_n. (d) The charge gap Δ_c.

the exact eigenstates for a range of F_0 are presented in Fig. 2(a) [Fig. 2(b)]. It turns out that either wave function provides a reasonably good approximation at sufficiently negative F_0. The maximal value achieved by Φ_1 is somewhat lower than that of Φ_2, but the former one performs better in a wider range of F_0. An important difference is that the overlap of Φ_2 increases monotonically as F_0 decreases but that of Φ_1 displays a weak peak around $F_0 \approx -0.38$. There is actually a third possibility

$$\Phi_3 = \chi_1(\{z\})\mathcal{P}_{\rm LLL}\{\chi_2(\{z\})[\chi_1(\{v\})\chi_1(\{w\})]\}, \qquad (12)$$

but we find that it does not have appreciable overlaps with exact eigenstates.

To establish incompressibility of the state, it is necessary to study the energy gaps of the system. For this purpose, the energy scale should be chosen properly. We have mentioned that the energy is expressed in units of $e^2/(\varepsilon\ell_B)$, but ℓ_B varies with the system size on the sphere. This problem can be remedied if we rescale the energy eigenvalues using the magnetic length in the thermodynamic limit [88–90]. The neutral gap

$$\Delta_n = E_1(N_e, 2N_e - 4) - E_0(N_e, 2N_e - 4) \qquad (13)$$

is shown in Fig. 2(c). It measures the energy difference between the first excited state, which belongs to a branch of collective magnetoroton modes [91–94], and the ground state. One can see a peak around $F_0 \approx -0.38$ in Fig. 2(c), which basically coincides with the relatively weak peak in Fig. 2(a). This implies that Φ_1 is a more reliable characterization of the exact ground state. The charge gap Δ_c is shown in Fig. 2(d). It is the energy cost associated with a well-separated quasiparticle-quasihole pair, which is closely related to the transport gap measured in experiments [88,89]. The appearance of a peak around $F_0 \approx -0.39$ in Fig. 2(d) again implies that Φ_1 is a better representation of the exact ground state. The neutral gap and charge gap have also been computed for $N_e = 14$ at $F_0 = -0.38$ using DMRG. As shown in Fig. 3, the gaps do not exhibit very good linear scaling versus $1/N_e$, but it is quite plausible that they saturate to finite values in the thermodynamic limit.

The parton interpretation also helps us to understand the edge physics [95]. It is helpful to recall some results in the hydrodynamic approach to quantum Hall edge physics. The edge wave is described by a one-dimensional density function $\rho(x)$ with the equation $\partial_t\rho + v\partial_x\rho = 0$. After canonical quantization, we obtain the $U(1)$ Kac-Moody algebra

$$[\rho(k), \rho(k')] = \nu\frac{k}{2\pi}\delta_{k+k'} \qquad (14)$$

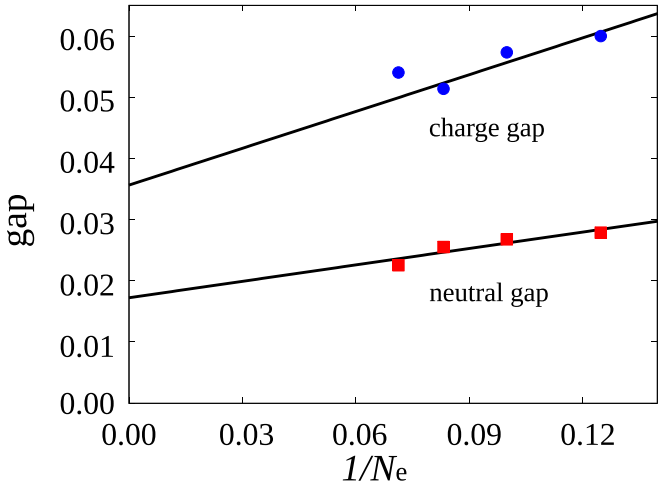

FIG. 3. Energy gaps Δ_n and Δ_c for the cases with $N_e = 8, 10, 12, 14$ at $F_0 = -0.38$. The lines are linear fits of the data points.

for the momentum space density function $\rho(k)$. In the parton construction, a subscript is introduced to distinguish the different types of partons, and the commutation relation becomes

$$[\rho_\lambda(k), \rho_\mu(k')] = \frac{k}{2\pi}\delta_{\lambda\mu}\delta_{k+k'}. \tag{15}$$

The partons in Eq. (8) have five edge modes: ρ_1 from $\chi_1(\{v\})$, ρ_2 from $\chi_1(\{w\})$, $\rho_{3,4}$ from $\chi_2(\{z\})$, and ρ_5 from $\chi_1(\{z\})$. These modes are not independent and they should be subjected to the constraint that relative density oscillations vanish [95]. To this end, we introduce an operator $\widetilde{\rho}_C = C_1(\rho_1 + \rho_2) + C_2(\rho_3 + \rho_4) + C_3\rho_5$. If $\sum_{\alpha=1}^{3} C_\alpha = 0$, $\widetilde{\rho}_C$ must commute with any physical operator because the fluctuations associated with $\widetilde{\rho}_C$ are unphysical. One can check that the edge density operators

$$j_0 = \sqrt{\frac{1}{2}}\left[\frac{1}{2}(\rho_1 + \rho_2) + \frac{1}{2}(\rho_3 + \rho_4) + \rho_5\right],$$
$$j_1 = \sqrt{\frac{1}{2}}(\rho_1 - \rho_2), \quad j_2 = \sqrt{\frac{1}{2}}(\rho_3 - \rho_4) \tag{16}$$

commute with $\widetilde{\rho}_C$, so the physical edge excitations have three branches. This means that the thermal Hall conductance of this state should be 3 in units of $\pi^2 k_B^2 T/(3h)$. It should be emphasized that our exploration of the edge physics is preliminary and things could be much more complicated in actual samples. If the confinement potential due to positive charges is not sharp enough in a system, its edge may be reconstructed such that additional modes are generated [96–102]. In the simplest scenario, edge reconstruction does *not* change the thermal Hall conductance. The presence of strong disorder further complicates things as electric and thermal transport properties could become sample-size dependent [103–105]. It is also desirable to search for other probes that can be used in combination with thermal Hall conductance. Shot noise has been proposed as a good indicator for the 5/2 state [106] and may also be useful in the current context.

Besides the parton state Eq. (8), there are two other celebrated two-component FQH states at filling factor 1/2. The first one is the Halperin 331 state [6]

$$\Phi_{331} = \prod_{j<k}(v_j - v_k)^3 \prod_{j<k}(w_j - w_k)^3 \prod_{j,k}(v_j - w_k) \tag{17}$$

with parent Hamiltonian

$$\sum_{i,j\in K^+} P_{ij}(1) + \sum_{i,j\in K^-} P_{ij}(1) + \sum_{i\in K^+, j\in K^-} P_{ij}(0). \tag{18}$$

The second one is the Haldane-Rezayi state [107]

$$\Phi_{\rm HR} = \mathrm{Det}\left[\frac{1}{(v_j - w_k)^2}\right]\prod_{j<k}(z_j - z_k)^2 \tag{19}$$

with parent Hamiltonian

$$\sum_{i,j\in K^\pm} P_{ij}(1). \tag{20}$$

We believe that they are not reasonable candidates for the $\nu = \pm 1/2$ states in graphene. One important reason that disfavors Φ_{331} is that it does not have the same SU(2) symmetry as the exact ground state. In previous studies, it has been found that Φ_{331} can be realized in bilayer systems when the interspecies interaction is reduced to some extent compared to the intraspecies interaction [49]. This scenario is also different from the graphene system because only the zeroth Haldane pseudopotential is reduced. The Haldane-Rezayi state can be constructed using nonunitary conformal field theory and it is most likely gapless in the thermodynamic limit [108–111]. The shift of Φ_{331} is 3 and that of $\Phi_{\rm HR}$ is 4, so the former cannot be compared directly with the parton state but the latter can. The two trial states with $N_e = 12$ have been generated numerically. The overlaps with the exact ground state are not impressive: the maximal value is 0.2339 for Φ_{331} (at $F_0 = -0.30$) and 0.4376 for $\Phi_{\rm HR}$ (at $F_0 = -0.40$). Thermal Hall conductance of the 331 state is 2 in units of $\pi^2 k_B^2 T/(3h)$, which can be used to distinguish it from the parton state in experiments. If the Haldane-Rezayi state is really gapless, there would be no quantized thermal Hall conductance.

IV. CONCLUSIONS

In conclusion, we propose that the $\nu = \pm 1/2$ states observed by Zibrov *et al.* [20] can be understood using the two-component parton wave function Eq. (8). This claim is supported by numerical calculations in a model of graphene with valley anisotropic interactions. The importance of valley anisotropic interactions calls for more in-depth studies. The parton framework can generate many non-Abelian FQH states and some of them may be experimentally relevant. It is natural to ask how to construct multicomponent non-Abelian FQH states using the parton theory and search for appropriate conditions to realize them. We hope that this paper will motivate further investigations of parton FQH states in various platforms.

ACKNOWLEDGMENTS

Exact diagonalization is performed using the DIAGHAM package, for which we are grateful to the authors. This work was supported by the National Natural Science Foundation of China under Grant No. 12174130.

[1] K. S. Novoselov, A. K. Geim, S. V. Morozov, D. Jiang, M. I. Katsnelson, I. V. Grigorieva, S. V. Dubonos, and A. A. Firsov, Two-dimensional gas of massless Dirac fermions in graphene, Nature (London) **438**, 197 (2005).

[2] Y. Zhang, Y.-W. Tan, H. L. Stormer, and P. Kim, Experimental observation of the quantum Hall effect and Berry's phase in graphene, Nature (London) **438**, 201 (2005).

[3] D. C. Tsui, H. L. Stormer, and A. C. Gossard, Two-Dimensional Magnetotransport in the Extreme Quantum Limit, Phys. Rev. Lett. **48**, 1559 (1982).

[4] R. B. Laughlin, Anomalous Quantum Hall Effect: An Incompressible Quantum Fluid with Fractionally Charged Excitations, Phys. Rev. Lett. **50**, 1395 (1983).

[5] F. D. M. Haldane, Fractional Quantization of the Hall Effect: A Hierarchy of Incompressible Quantum Fluid States, Phys. Rev. Lett. **51**, 605 (1983).

[6] B. I. Halperin, Theory of the quantized Hall conductance, Helv. Phys. Acta **56**, 75 (1983).

[7] J. K. Jain, Composite-Fermion Approach for the Fractional Quantum Hall Effect, Phys. Rev. Lett. **63**, 199 (1989).

[8] G. Moore and N. Read, Nonabelions in the fractional quantum Hall effect, Nucl. Phys. B **360**, 362 (1991).

[9] X. Du, I. Skachko, F. Duerr, A. Luican, and E. Y. Andrei, Fractional quantum Hall effect and insulating phase of Dirac electrons in graphene, Nature (London) **462**, 192 (2009).

[10] K. I. Bolotin, F. Ghahari, M. D. Shulman, H. L. Stormer, and P. Kim, Observation of the fractional quantum Hall effect in graphene, Nature (London) **462**, 196 (2009).

[11] C. R. Dean, A. F. Young, P. Cadden-Zimansky, L. Wang, H. Ren, K. Watanabe, T. Taniguchi, P. Kim, J. Hone, and K. L. Shepard, Multicomponent fractional quantum Hall effect in graphene, Nat. Phys. **7**, 693 (2011).

[12] B. E. Feldman, B. Krauss, J. H. Smet, and A. Yacoby, Unconventional sequence of fractional quantum Hall states in suspended graphene, Science **337**, 1196 (2012).

[13] D.-K. Ki, V. I. Fal'ko, D. A. Abanin, and A. F. Morpurgo, Observation of even denominator fractional quantum Hall effect in suspended bilayer graphene, Nano Lett. **14**, 2135 (2014).

[14] P. Maher, L. Wang, Y. Gao, C. Forsythe, T. Taniguchi, K. Watanabe, D. Abanin, Z. Papić, P. Cadden-Zimansky, J. Hone, P. Kim, and C. R. Dean, Tunable fractional quantum Hall phases in bilayer graphene, Science **345**, 61 (2014).

[15] A. Kou, B. E. Feldman, A. J. Levin, B. I. Halperin, K. Watanabe, T. Taniguchi, and A. Yacoby, Electron-hole asymmetric integer and fractional quantum Hall effect in bilayer graphene, Science **345**, 55 (2014).

[16] Y. Kim, D. S. Lee, S. Jung, V. Skákalová, T. Taniguchi, K. Watanabe, J. S. Kim, and J. H. Smet, Fractional quantum Hall states in bilayer graphene probed by transconductance fluctuations, Nano Lett. **15**, 7445 (2015).

[17] G. Diankov, C.-T. Liang, F. Amet, P. Gallagher, M. Lee, A. J. Bestwick, K. Tharratt, W. Coniglio, J. Jaroszynski, K. Watanabe, T. Taniguchi, and D. Goldhaber-Gordon, Robust fractional quantum Hall effect and composite fermions in the $n = 2$ Landau level in bilayer graphene, Nat. Commun. **7**, 13908 (2016).

[18] A. A. Zibrov, C. R. Kometter, H. Zhou, E. M. Spanton, T. Taniguchi, K. Watanabe, M. P. Zaletel, and A. F. Young, Tunable interacting composite fermion phases in a half-filled bilayer-graphene Landau level, Nature (London) **549**, 360 (2017).

[19] J. I. A. Li, C. Tan, S. Chen, Y. Zeng, T. Taniguchi, K. Watanabe, J. Hone, and C. R. Dean, Even denominator fractional quantum Hall state in bilayer graphene, Science **358**, 648 (2017).

[20] A. A. Zibrov, E. M. Spanton, H. Zhou, C. Kometter, T. Taniguchi, K. Watanabe, and A. F. Young, Even-denominator fractional quantum Hall states at an isospin transition in monolayer graphene, Nat. Phys. **14**, 930 (2018).

[21] Y. Kim, A. C. Balram, T. Taniguchi, K. Watanabe, J. K. Jain, and J. H. Smet, Evidence for a new even-denominator fractional quantum Hall state in graphene, Nat. Phys. **15**, 154 (2019).

[22] X. Liu, Z. Hao, K. Watanabe, T. Taniguchi, B. Halperin, and P. Kim, Interlayer fractional quantum Hall effect in a coupled graphene double-layer, Nat. Phys. **15**, 893 (2019).

[23] J. I. A. Li, Q. Shi, Y. Zeng, K. Watanabe, T. Taniguchi, J. Hone, and C. R. Dean, Pairing states of composite fermions in double-layer graphene, Nat. Phys. **15**, 898 (2019).

[24] K. Huang, H. Fu, D. R. Hickey, N. Alem, X. Lin, K. Watanabe, T. Taniguchi, and J. Zhu, Valley isospin controlled fractional quantum Hall states in bilayer graphene, Phys. Rev. X **12**, 031019 (2022).

[25] D. A. Abanin, B. E. Feldman, A. Yacoby, and B. I. Halperin, Fractional and integer quantum Hall effects in the zeroth Landau level in graphene, Phys. Rev. B **88**, 115407 (2013).

[26] I. Sodemann and A. H. MacDonald, Broken SU(4) Symmetry and the Fractional Quantum Hall Effect in Graphene, Phys. Rev. Lett. **112**, 126804 (2014).

[27] R. Willett, J. P. Eisenstein, H. L. Störmer, D. C. Tsui, A. C. Gossard, and J. H. English, Observation of an Even-Denominator Quantum Number in the Fractional Quantum Hall Effect, Phys. Rev. Lett. **59**, 1776 (1987).

[28] R. H. Morf, Transition from Quantum Hall to Compressible States in the Second Landau Level: New Light on the $\nu = 5/2$ Enigma, Phys. Rev. Lett. **80**, 1505 (1998).

[29] E. H. Rezayi and F. D. M. Haldane, Incompressible Paired Hall State, Stripe Order, and the Composite Fermion Liquid Phase in Half-Filled Landau Levels, Phys. Rev. Lett. **84**, 4685 (2000).

[30] M. Levin, B. I. Halperin, and B. Rosenow, Particle-Hole Symmetry and the Pfaffian State, Phys. Rev. Lett. **99**, 236806 (2007).

[31] S.-S. Lee, S. Ryu, C. Nayak, and M. P. A. Fisher, Particle-Hole Symmetry and the $\nu = \frac{5}{2}$ Quantum Hall State, Phys. Rev. Lett. **99**, 236807 (2007).

[32] M. R. Peterson, T. Jolicoeur, and S. Das Sarma, Finite-Layer Thickness Stabilizes the Pfaffian State for the 5/2 Fractional Quantum Hall Effect: Wave Function Overlap and Topological Degeneracy, Phys. Rev. Lett. **101**, 016807 (2008).

[33] M. R. Peterson, K. Park, and S. Das Sarma, Spontaneous Particle-Hole Symmetry Breaking in the $\nu = 5/2$ Fractional Quantum Hall Effect, Phys. Rev. Lett. **101**, 156803 (2008).

[34] A. E. Feiguin, E. Rezayi, K. Yang, C. Nayak, and S. Das Sarma, Spin polarization of the $\nu = 5/2$ quantum Hall state, Phys. Rev. B **79**, 115322 (2009).

[35] A. Wójs, C. Tőke, and J. K. Jain, Landau-Level Mixing and the Emergence of Pfaffian Excitations for the 5/2 Frac-

tional Quantum Hall Effect, Phys. Rev. Lett. **105**, 096802 (2010).

[36] M. Storni, R. H. Morf, and S. Das Sarma, Fractional Quantum Hall State at $\nu = \frac{5}{2}$ and the Moore-Read Pfaffian, Phys. Rev. Lett. **104**, 076803 (2010).

[37] K. Pakrouski, M. R. Peterson, T. Jolicoeur, V. W. Scarola, C. Nayak, and M. Troyer, Phase Diagram of the $\nu = 5/2$ Fractional Quantum Hall Effect: Effects of Landau-Level Mixing and Nonzero Width, Phys. Rev. X **5**, 021004 (2015).

[38] M. P. Zaletel, R. S. K. Mong, F. Pollmann, and E. H. Rezayi, Infinite density matrix renormalization group for multicomponent quantum Hall systems, Phys. Rev. B **91**, 045115 (2015).

[39] P. T. Zucker and D. E. Feldman, Stabilization of the Particle-Hole Pfaffian Order by Landau-Level Mixing and Impurities That Break Particle-Hole Symmetry, Phys. Rev. Lett. **117**, 096802 (2016).

[40] A. C. Balram, M. Barkeshli, and M. S. Rudner, Parton construction of a wave function in the anti-Pfaffian phase, Phys. Rev. B **98**, 035127 (2018).

[41] J. Yang, Particle-hole symmetry and the fractional quantum Hall states at 5/2 filling factor, arXiv:1701.03562.

[42] E. H. Rezayi, Landau Level Mixing and the Ground State of the $\nu = 5/2$ Quantum Hall Effect, Phys. Rev. Lett. **119**, 026801 (2017).

[43] R. V. Mishmash, D. F. Mross, J. Alicea, and O. I. Motrunich, Numerical exploration of trial wave functions for the particle-hole-symmetric Pfaffian, Phys. Rev. B **98**, 081107(R) (2018).

[44] L. Antonić, J. Vučičević, and M. V. Milovanović, Paired states at 5/2: Particle-hole Pfaffian and particle-hole symmetry breaking, Phys. Rev. B **98**, 115107 (2018).

[45] S. H. Simon, M. Ippoliti, M. P. Zaletel, and E. H. Rezayi, Energetics of Pfaffian–anti-Pfaffian domains, Phys. Rev. B **101**, 041302(R) (2020).

[46] E. H. Rezayi, K. Pakrouski, and F. D. M. Haldane, Stability of the particle-hole Pfaffian state and the $\frac{5}{2}$-fractional quantum Hall effect, Phys. Rev. B **104**, L081407 (2021).

[47] Y. W. Suen, L. W. Engel, M. B. Santos, M. Shayegan, and D. C. Tsui, Observation of a ν=1/2 Fractional Quantum Hall State in a Double-Layer Electron System, Phys. Rev. Lett. **68**, 1379 (1992).

[48] J. P. Eisenstein, G. S. Boebinger, L. N. Pfeiffer, K. W. West, and S. He, New Fractional Quantum Hall State in Double-Layer Two-Dimensional Electron Systems, Phys. Rev. Lett. **68**, 1383 (1992).

[49] S. He, S. Das Sarma, and X. C. Xie, Quantized Hall effect and quantum phase transitions in coupled two-layer electron systems, Phys. Rev. B **47**, 4394 (1993).

[50] V. W. Scarola and J. K. Jain, Phase diagram of bilayer composite fermion states, Phys. Rev. B **64**, 085313 (2001).

[51] M. R. Peterson and S. Das Sarma, Quantum Hall phase diagram of half-filled bilayers in the lowest and the second orbital Landau levels: Abelian versus non-abelian incompressible fractional quantum Hall states, Phys. Rev. B **81**, 165304 (2010).

[52] Z. Papić, M. O. Goerbig, N. Regnault, and M. V. Milovanović, Tunneling-driven breakdown of the 331 state and the emergent Pfaffian and composite Fermi liquid phases, Phys. Rev. B **82**, 075302 (2010).

[53] J. K. Jain, Incompressible quantum Hall states, Phys. Rev. B **40**, 8079 (1989).

[54] X.-G. Wen, Non-Abelian Statistics in the Fractional Quantum Hall States, Phys. Rev. Lett. **66**, 802 (1991).

[55] Y.-H. Wu, T. Shi, and J. K. Jain, Non-abelian parton fractional quantum Hall effect in multilayer graphene, Nano Lett. **17**, 4643 (2017).

[56] A. C. Balram, S. Mukherjee, K. Park, M. Barkeshli, M. S. Rudner, and J. K. Jain, Fractional Quantum Hall Effect at $\nu = 2 + 6/13$: The Parton Paradigm for the Second Landau Level, Phys. Rev. Lett. **121**, 186601 (2018).

[57] W. N. Faugno, A. C. Balram, M. Barkeshli, and J. K. Jain, Prediction of a Non-Abelian Fractional Quantum Hall State with f-Wave Pairing of Composite Fermions in Wide Quantum Wells, Phys. Rev. Lett. **123**, 016802 (2019).

[58] A. C. Balram, J. K. Jain, and M. Barkeshli, z_n superconductivity of composite bosons and the 7/3 fractional quantum Hall effect, Phys. Rev. Res. **2**, 013349 (2020).

[59] W. N. Faugno, J. K. Jain, and A. C. Balram, Non-abelian fractional quantum Hall state at 3/7-filled Landau level, Phys. Rev. Res. **2**, 033223 (2020).

[60] A. C. Balram, A non-Abelian parton state for the $\nu = 2 + 3/8$ fractional quantum Hall effect, SciPost Phys. **10**, 083 (2021).

[61] L. Belkhir and J. K. Jain, Theory of Spin-Singlet Fractional Quantum Hall Effect at $\upsilon = 1/2$, Phys. Rev. Lett. **70**, 643 (1993).

[62] L. Belkhir, X. G. Wu, and J. K. Jain, Half-integral spin-singlet quantum Hall effect, Phys. Rev. B **48**, 15245 (1993).

[63] M. Stern, P. Plochocka, V. Umansky, D. K. Maude, M. Potemski, and I. Bar-Joseph, Optical Probing of the Spin Polarization of the $\nu = 5/2$ Quantum Hall State, Phys. Rev. Lett. **105**, 096801 (2010).

[64] M. Stern, B. A. Piot, Y. Vardi, V. Umansky, P. Plochocka, D. K. Maude, and I. Bar-Joseph, NMR Probing of the Spin Polarization of the $\nu = 5/2$ Quantum Hall State, Phys. Rev. Lett. **108**, 066810 (2012).

[65] T. Tiemann, G. Gamez, N. Kumada, and K. Muraki, Unraveling the spin polarization of the ν=5/2 fractional quantum Hall state, Science **335**, 828 (2012).

[66] P. Wang, J. Sun, H. Fu, Y. Wu, H. Chen, L. N. Pfeiffer, K. W. West, X. C. Xie, and X. Lin, Finite-thickness effect and spin polarization of the even-denominator fractional quantum Hall states, Phys. Rev. Res. **2**, 022056(R) (2020).

[67] N. Moran, A. Sterdyniak, I. Vidanović, N. Regnault, and M. V. Milovanović, Topological d-wave pairing structures in Jain states, Phys. Rev. B **85**, 245307 (2012).

[68] S. Narayanan, B. Roy, and M. P. Kennett, Incompressible even denominator fractional quantum Hall states in the zeroth Landau level of monolayer graphene, Phys. Rev. B **98**, 235411 (2018).

[69] T. T. Wu and C. N. Yang, Dirac monopole without strings: monopole harmonics, Nucl. Phys. B **107**, 365 (1976).

[70] T. T. Wu and C. N. Yang, Some properties of monopole harmonics, Phys. Rev. D **16**, 1018 (1977).

[71] J. Jung and A. H. MacDonald, Theory of the magnetic-field-induced insulator in neutral graphene sheets, Phys. Rev. B **80**, 235417 (2009).

[72] C.-Y. Hou, C. Chamon, and C. Mudry, Deconfined fractional electric charges in graphene at high magnetic fields, Phys. Rev. B **81**, 075427 (2010).

[73] M. Kharitonov, Phase diagram for the $\nu = 0$ quantum Hall state in monolayer graphene, Phys. Rev. B **85**, 155439 (2012).

[74] I. F. Herbut, Theory of integer quantum Hall effect in graphene, Phys. Rev. B **75**, 165411 (2007).

[75] K. Nomura, S. Ryu, and D.-H. Lee, Field-Induced Kosterlitz-Thouless Transition in the $n = 0$ Landau Level of Graphene, Phys. Rev. Lett. **103**, 216801 (2009).

[76] F. Wu, I. Sodemann, Y. Araki, A. H. MacDonald, and T. Jolicoeur, SO(5) symmetry in the quantum Hall effect in graphene, Phys. Rev. B **90**, 235432 (2014).

[77] J. Lee and S. Sachdev, Wess-Zumino-Witten Terms in Graphene Landau Levels, Phys. Rev. Lett. **114**, 226801 (2015).

[78] S. R. White, Density Matrix Formulation for Quantum Renormalization Groups, Phys. Rev. Lett. **69**, 2863 (1992).

[79] U. Schollwöck, The density-matrix renormalization group in the age of matrix product states, Ann. Phys. (NY) **326**, 96 (2011).

[80] C. Hubig, I. P. McCulloch, and U. Schollwöck, Generic construction of efficient matrix product operators, Phys. Rev. B **95**, 035129 (2017).

[81] A. E. Feiguin, E. Rezayi, C. Nayak, and S. Das Sarma, Density Matrix Renormalization Group Study of Incompressible Fractional Quantum Hall States, Phys. Rev. Lett. **100**, 166803 (2008).

[82] J. Zhao, D. N. Sheng, and F. D. M. Haldane, Fractional quantum Hall states at $\frac{1}{3}$ and $\frac{5}{2}$ filling: Density-matrix renormalization group calculations, Phys. Rev. B **83**, 195135 (2011).

[83] Z.-X. Hu, Z. Papić, S. Johri, R. N. Bhatt, and P. Schmitteckert, Comparison of the density-matrix renormalization group method applied to fractional quantum Hall systems in different geometries, Phys. Lett. A **376**, 2157 (2012).

[84] M. P. Zaletel, R. S. K. Mong, and F. Pollmann, Topological Characterization of Fractional Quantum Hall Ground States from Microscopic Hamiltonians, Phys. Rev. Lett. **110**, 236801 (2013).

[85] G. Dev and J. K. Jain, Jastrow-Slater trial wave functions for the fractional quantum Hall effect: Results for few-particle systems, Phys. Rev. B **45**, 1223 (1992).

[86] X. G. Wu, G. Dev, and J. K. Jain, Mixed-Spin Incompressible States in the Fractional Quantum Hall Effect, Phys. Rev. Lett. **71**, 153 (1993).

[87] J. K. Jain and R. K. Kamilla, Composite fermions in the Hilbert space of the lowest electronic Landau level, Int. J. Mod. Phys. B **11**, 2621 (1997).

[88] G. Fano, F. Ortolani, and E. Colombo, Configuration-interaction calculations on the fractional quantum Hall effect, Phys. Rev. B **34**, 2670 (1986).

[89] N. d'Ambrumenil and R. Morf, Hierarchical classification of fractional quantum Hall states, Phys. Rev. B **40**, 6108 (1989).

[90] R. H. Morf, N. d'Ambrumenil, and S. Das Sarma, Excitation gaps in fractional quantum Hall states: An exact diagonalization study, Phys. Rev. B **66**, 075408 (2002).

[91] S. M. Girvin, A. H. MacDonald, and P. M. Platzman, Magneto-roton theory of collective excitations in the fractional quantum Hall effect, Phys. Rev. B **33**, 2481 (1986).

[92] S. He, S. H. Simon, and B. I. Halperin, Response function of the fractional quantized Hall state on a sphere. II. Exact diagonalization, Phys. Rev. B **50**, 1823 (1994).

[93] P. M. Platzman and S. He, Resonant Raman scattering from mobile electrons in the fractional quantum Hall regime, Phys. Rev. B **49**, 13674 (1994).

[94] K. Park and J. K. Jain, Two-Roton Bound State in the Fractional Quantum Hall Effect, Phys. Rev. Lett. **84**, 5576 (2000).

[95] X. G. Wen, Edge excitations in the fractional quantum Hall states at general filling fractions, Mod. Phys. Lett. B **05**, 39 (1991).

[96] A. H. MacDonald, S. R. E. Yang, and M. D. Johnson, Quantum dots in strong magnetic fields: Stability criteria for the maximum density droplet, Aust. J. Phys. **46**, 345 (1993).

[97] C. de C. Chamon and X. G. Wen, Sharp and smooth boundaries of quantum Hall liquids, Phys. Rev. B **49**, 8227 (1994).

[98] X. Wan, K. Yang, and E. H. Rezayi, Reconstruction of Fractional Quantum Hall Edges, Phys. Rev. Lett. **88**, 056802 (2002).

[99] Y. N. Joglekar, H. K. Nguyen, and G. Murthy, Edge reconstructions in fractional quantum Hall systems, Phys. Rev. B **68**, 035332 (2003).

[100] K. Yang, Field Theoretical Description of Quantum Hall Edge Reconstruction, Phys. Rev. Lett. **91**, 036802 (2003).

[101] J. Wang, Y. Meir, and Y. Gefen, Edge Reconstruction in the $\nu = 2/3$ Fractional Quantum Hall State, Phys. Rev. Lett. **111**, 246803 (2013).

[102] R. Sabo, I. Gurman, A. Rosenblatt, F. Lafont, D. Banitt, J. Park, M. Heiblum, Y. Gefen, V. Umansky, and D. Mahalu, Edge reconstruction in fractional quantum Hall states, Nat. Phys. **13**, 491 (2017).

[103] C. L. Kane, M. P. A. Fisher, and J. Polchinski, Randomness at the Edge: Theory of Quantum Hall Transport at Filling $\nu = 2/3$, Phys. Rev. Lett. **72**, 4129 (1994).

[104] J. E. Moore and X.-G. Wen, Classification of disordered phases of quantum Hall edge states, Phys. Rev. B **57**, 10138 (1998).

[105] I. V. Protopopov, Y. Gefen, and A. D. Mirlin, Transport in a disordered $\nu = 2/3$ fractional quantum Hall junction, Ann. Phys. (NY) **385**, 287 (2017).

[106] J. Park, C. Spånslätt, Y. Gefen, and A. D. Mirlin, Noise on the non-Abelian $\nu = 5/2$ fractional quantum Hall edge, Phys. Rev. Lett. **125**, 157702 (2020).

[107] F. D. M. Haldane and E. H. Rezayi, Spin-Singlet Wave Function for the Half-Integral Quantum Hall Effect, Phys. Rev. Lett. **60**, 956 (1988).

[108] V. Gurarie, M. Flohr, and C. Nayak, The Haldane-Rezayi quantum Hall state and conformal field theory, Nucl. Phys. B **498**, 513 (1997).

[109] N. Read and D. Green, Paired states of fermions in two dimensions with breaking of parity and time-reversal symmetries and the fractional quantum Hall effect, Phys. Rev. B **61**, 10267 (2000).

[110] M. Hermanns, N. Regnault, B. A. Bernevig, and E. Ardonne, From irrational to nonunitary: Haffnian and Haldane-Rezayi wave functions, Phys. Rev. B **83**, 241302(R) (2011).

[111] V. Crépel, N. Regnault, and B. Estienne, Matrix product state description and gaplessness of the Haldane-Rezayi state, Phys. Rev. B **100**, 125128 (2019).